Growth mechanism of thin oxide films under low-energy oxygen-ion bombardment

S. S. Todorov[a] and E. R. Fossum
Department of Electrical Engineering and Columbia Radiation Laboratory, Columbia University, New York, New York 10027

(Received 24 September 1987; accepted 20 October 1987)

Bombardment of silicon surfaces by low-energy oxygen ions has been investigated as a possible process for growing films of SiO_2 at room temperature. Broad ion beams of energy 40–200 eV and variable oxygen content have been used to grow ultrathin oxides of extremely uniform thickness. The ion beam oxides are similar to thin thermal oxides in many respects—composition, chemical binding, optical, and electrical properties. The dependence of the thickness and quality of the oxide films on ion dose, ion energy, and substrate temperature have been investigated. The obtained thickness is observed to vary only slightly with increasing substrate temperature up to 650 °C which indicates nonthermal process kinetics. The ion-beam oxides reach a limiting thickness of 40–60 Å which is largely independent of ion dose and is also found to be insensitive to ion energy. The observed oxidation is explained on the basis of surface implantation and radiation-enhanced diffusion and reaction processes. Limited thicknesses are observed even when sputtering is negligible because of the decreasing effective penetration of the ions due to the swelling of the target which accompanies the conversion of Si to SiO_2. Thus the film grows until the oxide–semiconductor interface moves beyond the current-ion penetration depth after which oxidation effectively stops. This model is equally applicable to high-energy, high-dose oxygen-ion implantation for production of buried oxides in silicon-on-insulator technology where it is observed that oxide growth occurs predominantly at the upper interface.

I. INTRODUCTION

Further advances in the development of high-density integrated circuits (ICs) will require scaled-down device dimensions, closer device packing, and a greater number of fabrication steps. These in turn require reduced IC fabrication thermal budgets and, in the case of metal–oxide–semiconductor (MOS) devices, thinner gate dielectrics. The trend toward larger substrates places an additional requirement on the lateral uniformity of the gate oxides. The problem of obtaining high-quality thin films of SiO_2 at reduced temperatures has been approached from two directions—oxide growth and oxide deposition. These differ in the type of material being supplied to the substrate–oxygen only or both oxygen and silicon. Both approaches rely on the use of some form of energetic species to enhance the low oxidation rates typically observed at reduced temperatures. Successful fabrication of MOS devices has been reported for gate dielectrics grown by plasma oxidation at 500–600 °C[1,2] and deposited by rf sputtering at 200–300 °C.[3] Very thin SiO_2 films of high electrical quality have also been deposited by plasma-enhanced chemical vapor deposition (PE-CVD) at 350 °C.[4] MOS transistors have been fabricated using very thin gate dielectrics grown at 25 °C by ion beam oxidation.[5]

Due to the spatial separation of the plasma producing region and the sample, ion beam oxidation permits independent control over ion energy and ion flux, substrate temperature, and angle of incidence. These in turn permit detailed study of the influence of the different process parameters on the obtained oxides, the results of which may be extended to rf oxidation.

The electrical characteristics and other properties of the very thin oxide films grown at room temperature by ion beam oxidation have been reported previously.[5,6] Briefly, these showed that ion beam oxides are similar to thermally grown SiO_2 films of equal thickness in many respects. They have almost identical Auger sputter profiles except for the apparently sharper interface of the thermal oxide. X-ray photoelectron spectroscopy at glancing detector angles indicated the presence of lower oxides of silicon at the film surface. The most notable difference between thermal and ion beam oxides is the two to three orders of magnitude greater leakage current in reverse bias for the latter. However, this leakage was another three orders of magnitude lower than the drain–source saturation current and thus did not degrade metal–oxide–semiconductor field effect transistor (MOSFET) performance.[5] In this paper we will discuss the dependence of the oxide growth kinetics on the ion bombardment conditions and will propose a mechanism describing the oxidation process.

II. EXPERIMENT

The test vehicles are (100) silicon wafers, 5-cm diameter, polished on the side. Both *p*- and *n*-type wafers of resistivity 2–5 Ω cm are used. The samples are prepared by chemical cleaning and the growth and stripping of two thick 900 °C oxides after which they are loaded into the ion-beam processing chamber. Ion beam oxidation is performed using a single-grid broad-beam ion source, described previously.[7] The source operates on a mixture of argon and oxygen. It was found that a 1:1 $Ar:O_2$ ratio allowed both good control over source operation for extended periods of time and led to

 0734-211X/88/010466-04$01.00

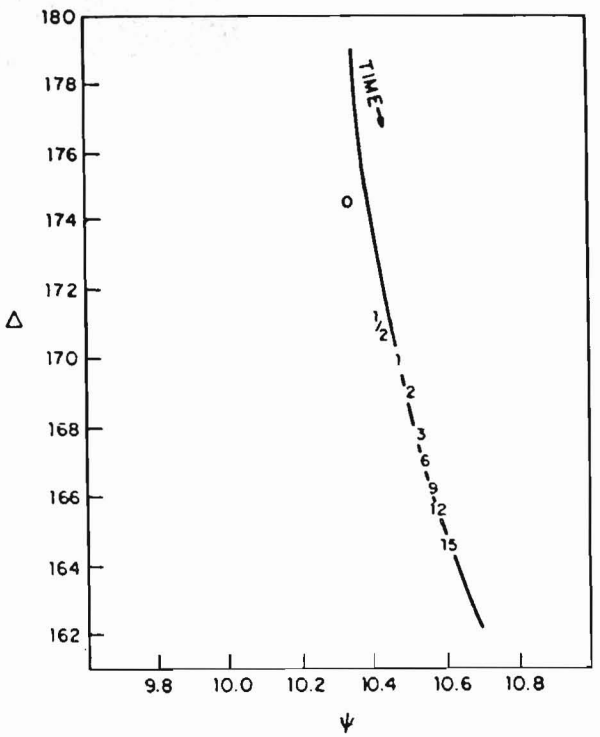

FIG. 1. Comparison of the evolution of thin 875 °C thermal (solid line) and 25 °C ion beam (numbers) oxide films. The numbers correspond to the exposure in minutes to a 60 eV ion beam of 1:1 $Ar:O_2$ content and an oxygen dose rate of 5×10^{16} cm^{-2} min^{-1}.

the production of oxide films on the substrates. After unloading from the ion-beam processing chamber the thickness of the obtained films is measured with a Gaertner L117 ellipsometer using a He–Ne laser. The thicknesses measured by ellipsometry correlate well with those obtained by Auger sputter profiling, calculated from the ratio of the x-ray photoelectron spectroscopy (XPS) Si 2p peaks or calculated from the capacitance–voltage characteristics of MOS capacitors.[6] The oxide thickness was calculated from the ellipsometer measurements with the standard *a priori* assumption of the refractive index necessary for ultrathin films. The index of refraction used is that of thermal SiO_2. This is justified by the aforementioned similarity between the two types of oxides, further illustrated in Fig. 1 which compares the unprocessed ellipsometer parameters Δ and ψ. The solid line shows the evolution of Δ and ψ for thermal oxides of increasing thickness grown at 875 °C. The numbers represent ion beam oxides and correspond to the oxygen ion dose received during the exposure. The ion-beam current density was 135 $\mu A/cm^2$ which corresponds to a flux rate of 5×10^{16} O/cm^2 min. It is clear that the two oxides evolve along essentially the same lines pointing further to their similarity.

III. RESULTS AND DISCUSSION

The dependence of the obtained ion-beam oxide thickness on oxygen ion dose is presented in Fig. 2. The silicon wafers were bombarded by a 60-eV ion beam containing O_2 and Ar in a 1:1 ratio. The substrate temperature was monitored by a substrate holder mounted thermocouple and is 25 °C. The figure shows that there is an approximate logarithmic depen-

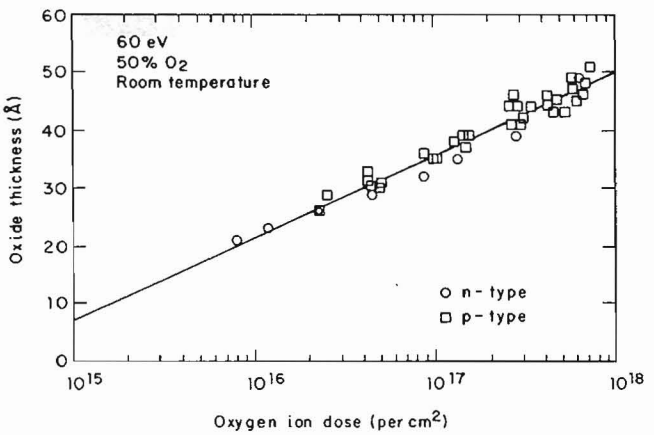

FIG. 2. Ion-beam oxide thickness as a function of oxygen dose. Ion energy: 60 eV. Beam oxygen content: 50%. Substrate temperature: 25 °C. (□) *p*-type silicon; (○) *n*-type silicon.

dence on the oxygen ion dose though the scatter in the data is more pronounced at higher doses. The scatter is attributed to instabilities in the ion source which become more important at the long exposure times necessary to achieve high doses. It appears that the *n*-type wafers oxidize somewhat more slowly than the *p*-type wafers, however, the differences are within the experimental uncertainty. It has been observed previously that the ion beam oxides exhibit very good thickness uniformity over the surface of the wafer even though they are grown by an ion beam which has a peaked Gaussian-like profile.[5] This insensitivity to oxygen ion dose was attributed to the attaining of a self-limiting value of the thickness. While it is now clear that such self-limiting behavior is not being observed, it is also clear that the growth rate at high doses is sufficiently low so that even twofold increases in the ion dose would lead to the growth of only about a monolayer of oxide.

Self-limiting oxide growth has been observed in the case of rf oxidation of lead[8] and ion beam oxidation of nickel.[9] It is attributed to the achieved balance between the competing processes oxidation and sputtering. The oxidation rate is initially large and decreases with increasing film thickness whereas the sputtering rate is independent of oxide thickness. Thus the oxide growth will stop at a thickness value at which the two rates become equal.

It is expected that self-limitation will occur earlier at higher ion beam energies where sputtering is more pronounced. That is indeed the case as shown in Fig. 3. The samples are bombarded with a 100-eV ion beam with a 1:1 O_2:Ar ratio at 25 °C. It is seen that at higher ion energies higher initial oxidation rates are observed. This is probably related to the greater depths at which the ions are stopped and the increased probability that they will be retained in the target. The oxidation rate then decreases more quickly than for 60 eV ions and appears to exhibit self-limiting behavior.

To investigate the importance of beam heating of the substrate during ion bombardment several samples were oxidized at different oxygen dose rates leading to the same received dose. The ion flux at the substrate was varied by changing the source discharge power or by changing the sorce-to-substrate distance. No differences in the properties of the obtained oxides were observed.

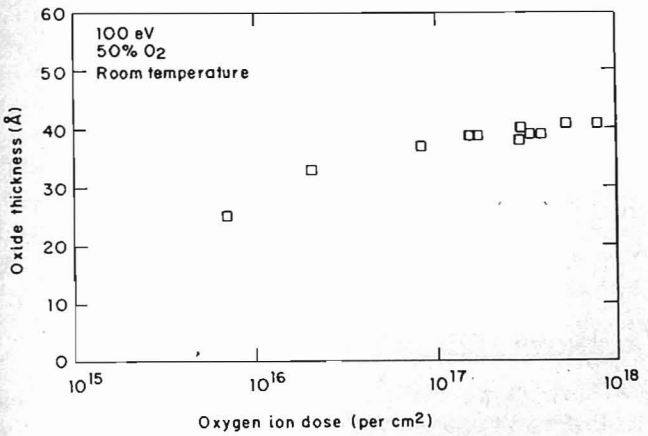

FIG. 3. Ion-beam oxide thickness as a function of oxygen dose. Ion energy: 100 eV. Beam oxygen content: 50%. Substrate temperature: 25 °C. (□) *p*-type silicon.

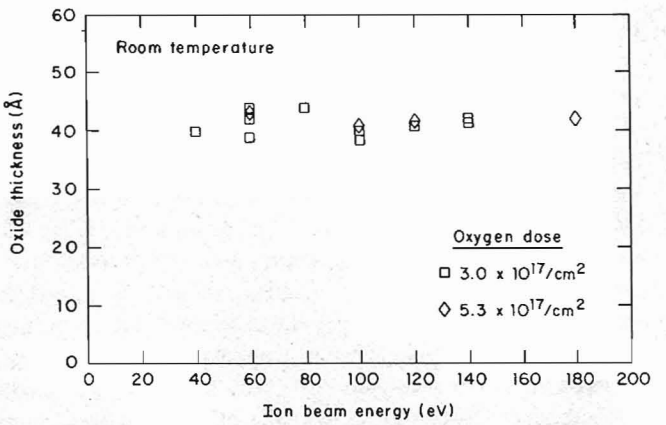

FIG. 5. Ion-beam oxide thickness as a function of ion energy. Beam oxygen content: 50%. Substrate temperature: 25 °C. (□) O dose: 3.0×10^{17} cm^{-2}. (◇) O dose: 5.3×10^{17} cm^{-2}.

The substrate may be intentionally heated up to 650 °C by means of resistive heating of the substrate holder. The obtained oxide thickness for fixed ion beam conditions is observed to increase with increasing substrate temperature. However, this dependence is rather weak, especially considering the large temperature range. Presenting the data in an Arrhenius plot, as shown in Fig. 4, allows the extraction of an activation energy E_{act} for the process. Here the oxidation rate dependence has been approximated by $x = C \ln t$, where t is the oxidation time and C is a constant which is assumed to depend on the temperature T in the standard fashion: $C = C_0 \exp(-E_{act}/kT)$, where k is the Boltzmann constant. Note that the data are largely independent of ion dose. The slope of the obtained straight line allows the determination of $E_{act} = 7$ meV. For comparison the activation energy of the linear rate constant B/A defined in thermal oxidation of silicon is 2 eV.[10] Clearly, oxidation due to ion bombardment relies on nonthermal mechanisms of enhancing the diffusivity and reactivity of the oxidizing species.

The observed oxide thicknesses are similar to the expected oxygen ion projected range, accounting for the volume expansion which accompanies the conversion of silicon to SiO_2. Thus, from a surface implantation perspective the obtained thickness may be expected to increase at higher ion energies. The dependence of oxide thickness on ion energy for a fixed oxygen ion dose is shown in Fig. 5 for beams with a 50% oxygen content. The lack of a trend over the covered energy range is evident. It is likely that the increased oxidation rate is counteracted by an increase in the sputtering yield since both processes are governed by similar mechanisms.

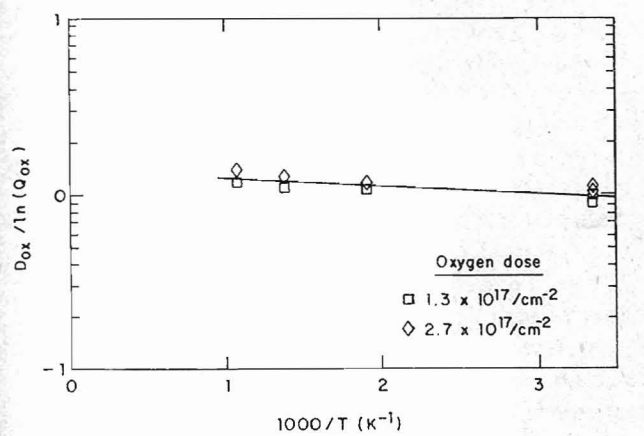

FIG. 4. Arrhenius plot for logarithmic ion beam oxidation rate constant. Ion energy: 60 eV. Beam oxygen content: 50%. (□) O dose: 1.3×10^{17} cm^{-2}. (◇) O dose: 2.7×10^{17} cm^{-2}.

IV. PROCESS MODEL

Previous models of low-energy ion-beam oxidation of metals described the oxidation process in the absence of sputtering as descreasing exponentially with increasing exposure time.[9] However, this model is carried over from the process of rf oxidation of metals in which a self-biasing of the oxide layer is observed[8,11] and does not account for the fact that the oxidizing species are actually deposited below the surface and are distributed throughout the film. Also it does not explain the observed enhancement in the oxidation rates over thermal oxidation processes.

It is considered appropriate to view low-energy ion-beam oxidation of silicon as a scaled-down version of the high-energy high-dose oxygen-implantation processes used for obtaining buried layers of SiO_2 in silicon-on-insulator (SOI) technology. The models developed to describe this process introduce an enhanced effective diffusion constant and reaction rate and also take into account the swelling of the target.[12,13] These models, however, neglect any spatial dependence of the enhancement and lead to the prediction of preferential growth toward the substrate.[12] It has been observed that the growth of the buried oxide layer takes place mostly at the top interface.[14,15] The preferred oxidation upwards has been attributed to the different fate of silicon interstitials at the two Si–SiO_2 interfaces.[16] The interstitials which are emitted during the oxidation process can recombine at defects or at the surfaces of the wafer. Due to the much larger distance to the back surface, the interstitials at the bottom interface are practically fixed and serve to block the oxidation process.[16]

We propose an important modification to these models. While it is clear that sputtering and oxidation compete for

domination in these processes, the explanation of enhanced oxidation in unheated substrates is considered unsatisfactory. It is proposed that the enhanced reactivity and mobility of the oxidizing species are due to the ion bombardment. Thus, at any time, oxidation is taking place only at those depths which are currently being reached by the ion beam. The swelling which accompanies the conversion of silicon to silicon dioxide effectively prevents later ion arrivals from reaching the same depths in the silicon. Moreover, it is difficult for them to diffuse deeper into the substrate after they are stopped since their diffusion is enhanced only in the region in which the ions are depositing energy. In other words, it is important to recognize that the effective process rates are spatially dependent. Because of the volume expansion this spatial dependence means that the oxidation rate at the oxide–semiconductor interface is time dependent and oxidation at the lower interface will stop when a sufficient portion of the substrate has been converted to SiO_2. Note that the concept of a temperature increase due to thermal spikes or beam heating is not necessary for this treatment. Enhanced mobility and reactivity may be due to other beam related processes like the creation of excess numbers of defects in the vicinity of an atom or the transfer of excess energy to the atom in a collision.[17]

The proposed model accounts for the enhanced oxidation rates observed for unheated substrates under ion bombardment. Also, it accounts for the insensitivity to substrate temperature observed in experiments on low-energy ion-beam oxidation of silicon. Further, it naturally explains the limited thicknesses observed with this technique even in the absence of sputtering. The model is simply extended to the preferred growth toward the top surface of the wafer observed in the case of buried oxides produced by high energy oxygen implantation. A quantitative evaluation of the process parameters based on this model will be published separately.[18]

V. CONCLUSION

In summary the bombardment of silicon surfaces by low-energy oxygen-ion beams is observed to lead to the growth of ultrathin films of silicon dioxide. The oxide growth is self-limiting due to the competing processes of surface implantation and sputtering. Limited thicknesses are also observed in the absence of sputtering. The oxidation reaction process is explained in terms of beam-enhanced reactivity and mobility of the oxidizing species. The importance of recognizing the spatial limitations of the enhanced oxidation process is stressed. The explanation of the process is extended to buried SiO_2 layers produced by oxygen implantation.

ACKNOWLEDGMENT

This work was performed under Joint Services Electronics Program Contract No. DAAG-29-85-K-0049.

[a] Permanent Address: Institute of Electronics, Sofia, Bulgaria.

[1] A. K. Ray and A. Reisman, J. Electrochem. Soc. **128**, 2424 (1981).
[2] S. I. Kimura, E. Murakami, T. Warabisako, H. Sunami, and T. Tokuyama, IEEE Electron Device Lett. **7**, 38 (1986).
[3] H. S. Lee and S. C. Chang, IEEE Electron Device Lett. **3**, 310 (1982).
[4] J. Batey, E. Tierney, and T. N. Nguyen, IEEE Electron Device Lett. **8**, 148 (1987).
[5] S. S. Todorov, S. L. Shillinger, and E. R. Fossum, IEEE Electron Device Lett. **7**, 468 (1986).
[6] C. F. Yu, S. S. Todorov, and E. R. Fossum, J. Vac. Sci. Technol. A **5**, 1569 (1987).
[7] S. S. Todorov, C. F. Yu, and E. R. Fossum, Vacuum **36**, 929 (1986).
[8] J. H. Greiner, J. Appl. Phys. **42**, 5151 (1971).
[9] J. M. E. Harper, M. Heiblum, J. L. Speidell, and J. J. Cuomo, J. Appl. Phys. **52**, 4118 (1981).
[10] B. E. Deal, J. Electrochem. Soc. **110**, 122 (1979).
[11] A. T. Fromhold and M. Baker, J. Appl. Phys. **51**, 6377 (1980).
[12] H. U. Jager, E. Hensel, U. Kreissig, W. Skorupa, and E. Sobeslavsky, Thin Solid Films **123**, 159 (1985).
[13] E. A. Maydell-Ondrusz and I. H. Wilson, Thin Solid Films **114**, 357 (1984).
[14] T. Hayashi, H. Okamoto, and Y. Homma, Jpn. J. Appl. Phys. **19**, 1005 (1980); T. Hayashi, S. Maeyama, and S. Yoshii, *ibid.* **19**, 1111 (1980).
[15] J. A. Kilner, R. J. Chater, P. L. F. Hemment, R. F. Peart, E. A. Maydell-Ondrusz, M. R. Taylor, and R. P. Arrowsmith, Nucl. Instrum. Methods. B **7/8**, 293 (1985).
[16] A. H. van Ommen, B. H. Koek, and M. P. A. Viegers, Appl. Phys. Lett. **49**, 628 (1986).
[17] S. M. Myers, Nucl. Instrum. Methods. **168**, 265 (1980).
[18] S. S. Todorov and E. R. Fossum, Appl. Phys. Lett. **52**, 48 (1988).